Flow of Two-Immiscible Fluids in Porous and Nonporous Channels

Ali J. Chamkha
Associate Professor,
Department of Mechanical and Industrial Engineering,
Kuwait University,
P.O. Box 5969,
Safat, 13060 Kuwait

This study considers steady, laminar flow of two viscous, incompressible, electrically-conducting and heat-generating or absorbing immiscible fluids in an infinitely-long, impermeable parallel-plate channel filled with a uniform porous medium. A magnetic field of uniform strength is applied normal to the flow direction. The channel walls are assumed to be electrically nonconducting and are maintained at two different temperatures. When present, the porous medium is assumed to act as an electrical insulator and that it is in local thermal equilibrium with the fluid. The transport properties of both fluids are assumed to be constant. This study is expected to be useful in understanding the influence of the presence of slag layers on the flow and heat transfer aspects of coal-fired Magnetohydrodynamic (MHD) generators when the porous medium is absent and the effects of thermal buoyancy and a magnetic field on enhanced oil recovery and filtration systems where the porous medium is present. The problem is formulated by employing the balance laws of mass, linear momentum, and energy for both phases. Continuous conditions for the velocity and temperature as well as the shear stress and heat flux of both phases at the interface are employed. The resulting governing ordinary differential equations are solved numerically subject to the boundary and interface conditions for the velocity and temperature distributions of both fluids in the channel. Analytical solutions for a special case of the problem where the porous medium is absent or only its inertia effect is neglected are obtained. Comparisons with previously reported velocity profiles are performed and excellent agreements are obtained. A parametric study illustrating the influence of the physical parameters involved in the problem is conducted and the results are presented graphically and discussed. [S0098-2202(00)02101-5]

Introduction

The possibility of power generation from magnetohydrodynamic (MHD) coal-fired generators coated with a coal slag layer has increased interest in understanding the behavior of slag layers in MHD generator ducts (Pian and Smith [1]). In addition, the use of electrically-conducting and heat generating or absorbing fluids such as liquid metals as heat transfer agents in MHD power generation devices and nuclear engineering systems has created a growing interest in studying the influence of magnetic fields on such fluids and the subsequent effect on the efficiency of these devices and systems. Shail [2] studied MHD flow of a conducting fluid in a channel with a layer of nonconducting fluid between the upper channel wall and the conducting fluid. As a result of this study, Shail [2] reported that an increase of the order of 30% can be achieved in the flow rate of an electromagnetic pump for suitable depth and viscosity ratios of the two fluids and realistic values of the Hartmann number.

Thome [3] initiated the first investigation associated with two-phase liquid metal magneto-fluid-mechanics generator. Postlethwaite and Sluyter [4] presented an overview of the heat transfer problems related to MHD generators. Lohrasbi and Sahai [5] considered MHD two-phase flow and heat transfer in a horizontal parallel-plate channel and reported analytical solutions for the velocity and temperature profiles for the case where only one of the fluids is electrically conducting. Malashetty and Leela [6,7] reported closed-form solutions for the two-phase flow and heat transfer situation in a horizontal channel for which both phases are electrically conducting. Recently, Malashetty and Umavathi [8] studied two-phase MHD flow and heat transfer in an inclined channel in the presence of buoyancy effects for the situation where only one of the phases is electrically conducting. All of the studies referenced above are useful in understanding the effect of the presence of slag layers on the heat transfer aspects of coal-fired MHD generators.

A more realistic analysis of slag layers in coal-fired MHD generators is not easy in view of the vast variations in the physical properties of the slag with temperature and the difficult-to-handle wall boundary conditions. Nevertheless, the results of very idealized situations can show some aspects of the physics involved in the problem.

The corresponding porous medium channel problem finds many important applications in geothermal and geophysical engineering such as underground disposal of nuclear wastes, spreading of chemical pollutants in water-saturated soil, migration of moisture in fibrous insulation, structure reaction and gas assisted injection molding, die filling processes, clean-up of refineries and extraction of geothermal energy. For example, in the recovery of hydrocarbons from underground petroleum deposits, the use of thermal process is becoming very important as it enhances the recovery. In this case, heat is injected into the reservoir through hot water or steam or it can be generated by burning part of the crude oil in the reservoir. In all such thermal recovery processes, the flow of the immiscible fluids with heat generation takes place through a porous medium and the free convection currents are detrimental (Hiremath and Patil [9]).

Most early works on porous media have used the Darcy law which represents an empirical relation between the Darcian velocity and the pressure drop across the porous medium. Vafai and Tien [10] have discussed the importance of boundary and inertia effects of porous media which are not accounted for by the Darcy law. Plumb and Huenefeld [11] have also discussed the non-Darcian porous medium effects in their work on natural convection from heated surfaces in porous media. Nakayama et al. [12] have reported exact and approximate solutions through an analysis on forced convection in a channel filled with a Brinkman-Darcy porous medium. Renken and Poulikakos [13] presented an experimental investigation of forced convective heat transport in a packed bed of spheres occupying a heated channel. Also, Vafai

Contributed by the Fluids Engineering Division for publication in the JOURNAL OF FLUIDS ENGINEERING. Manuscript received by the Fluids Engineering Division November 16, 1998; revised manuscript received December 6, 1999. Associate Technical Editor: M. Sommerfeld.

and Kim [14] have studied and reported an exact solution for forced convection in a channel filled with a porous medium. More recently, Srinivasan and Vafai [15] have reported a theoretical study for predicting the movement of the interface for linear encroachment in two immiscible fluid systems in a porous medium taking into account the non-Darcian boundary and inertia effects. Chen and Vafai [16,17] have analyzed free surface momentum and energy transport in porous media in the absence and presence of surface tension effects.

Along these lines, it is the objective of this paper to consider the problem of flow and heat transfer of two electrically-conducting and heat generating or absorbing immiscible fluids in a vertical infinitely long channel in the presence or absence of a porous medium and applied magnetic field. Both fluids and the porous medium are in local thermal equilibrium. The magnetic Reynolds number is assumed to be small so that the induced magnetic field will be neglected. This assumption results in uncoupling of the balance of linear momentum and Maxwell equations (see Cramer and Pai [18]). In addition, no electric field is assumed to exist (short circuit) and the effects of viscous dissipation, Joule heating, are neglected. This is done in order to focus on the effects of heat generation or absorption, buoyancy currents and the porous medium effects.

Problem Formulation

Consider steady, laminar, hydromagnetic, fully developed flow of two immiscible fluids in a channel of infinitely long vertical walls extending in the x and z directions filled with a uniform porous medium and in the presence of natural convection currents. Both walls of the channel are maintained at different temperatures T_{w1} and T_{w2} and are electrically nonconducting. One of the fluids (Fluid 1) occupies the region $0 \leqslant y \leqslant h_1$, and the other fluid (Fluid 2) occupies the region $-h_2 \leqslant y \leqslant 0$. Both fluids are assumed to be Newtonian, electrically conducting, and heat generating or absorbing and have constant properties except the density in the buoyancy terms of the momentum equations. A magnetic field of uniform strength is applied in the y direction normal to the direction of flow. Constant magnetic fields are used in most controlled experiments and applications. For this reason and to allow for the possibility of analytical solutions, this assumption is retained here. The schematics of the problem and the coordinate system are shown in Fig. 1. The governing equations for this investigation are based on the balance laws of mass, linear momentum, and energy of both phases and the boundary and interface conditions. Under the assumptions stated above, and taking into account the Boussinesq approximation, the governing equations can be written as

$$\mu_{e1}\frac{d^2u_1}{dy_1^2}+\rho_1 g\beta_1(T_1-T_0)=\frac{\partial p}{\partial x}+\sigma_1 B_0^2 u_1+\frac{\mu_1}{K}u_1+\rho_1 C_F u_1^2 \tag{1}$$

$$k_1\frac{d^2T_1}{dy_1^2}\pm Q_1(T_1-T_0)=0 \tag{2}$$

$$\mu_{e2}\frac{d^2u_2}{dy_2^2}+\rho_2 g\beta_2(T_2-T_0)=\frac{\partial p}{\partial x}+\sigma_2 B_0^2 u_2+\frac{\mu_2 u_2}{K}+\rho_2 C_F u_2^2 \tag{3}$$

$$k_2\frac{d^2T_2}{dy_2^2}\pm Q_2(T_2-T_0)=0 \tag{4}$$

where x and y_i $(i=1,2)$ are the vertical and normal (for Fluids 1 and 2) directions, respectively. u_1 and T_1 are the x-velocity component and temperature of Fluid 1, respectively. ρ_1, μ_{e1}, μ_1, β_1, σ_1, and $Q_1\,(>0)$ are the density, effective dynamic viscosity, dynamic viscosity, coefficient of thermal expansion, electrical conductivity and heat generation or absorption coefficient for Fluid 1, respectively. $-\partial p/\partial x$, g, T_0, and B_0 are the pressure gradient, gravitational acceleration, reference temperature, and magnetic induction, respectively. K, C_F, and k are the porous medium permeability, inertia coefficient, and the effective thermal conductivity, respectively. Variables and properties with subscript 2 correspond to Fluid 2. Brinkman in his extension of the Darcy law made the assumption that $\mu_e=\mu$. Therefore, for simplicity, this will be adopted herein.

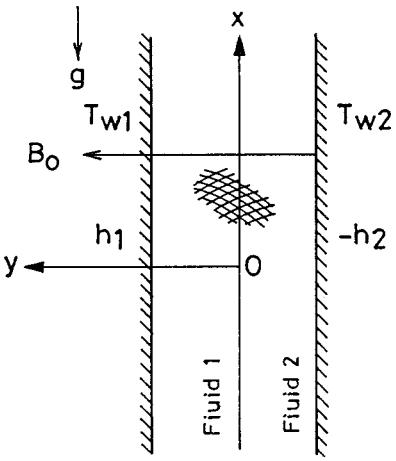

Fig. 1 Model schematic and coordinate system

It is seen from Eqs. (1) and (3) that both fluids share a common pressure gradient. Also, the convective transport terms in Eqs. (2) and (4) are neglected since the temperatures of the walls are constant. This can be verified by differentiating both Eqs. (1) and (3) with respect to x. It should be mentioned that the positive signs before Q_1 and Q_2 correspond to heat generation of both fluids while the negative signs before Q_1 and Q_2 correspond to heat absorption of both fluids. Also, it is seen that the heat generation or absorption effects are assumed to be temperature dependent as done by Sparrow and Cess [19], Vajravelu and Nayfeh [20], Vajravelu and Hadjinicolaou [21], and Chamkha [22]. Examples of heat generation in fluids are abundant, for instance, heating of flowing water in a solar collector and radiative cooling of molten glass in a forehearth. Also, electric current in semi-conducting fluids such as glass and electrolyte generate Joulean heating (Song [23]). Other applications include those involving exothermic and endothermic chemical reactions and dealing with dissociating fluids (Vajravelu and Nayfeh [20]).

It should be noted that the stratified two-phase flow in the vertical porous channel is due to mixed convection. Generally speaking, for such a configuration in natural convection the flow is contrarotative: upward along the hot surface and downward along the cold surface. However, in mixed convection, the flow is either upward or downward depending on the relative influence of the natural convection effect caused by thermal buoyancy and the forced convection effect caused by the applied pressure gradient.

The boundary and interface conditions for this problem can be written as

$$u_1(h_1)=0, \tag{5a}$$

$$T_1(h_1)=T_{w1}, \tag{5b}$$

$$u_2(-h_2)=0, \tag{5c}$$

$$T_2(-h_2)=T_{w2} \tag{5d}$$

$$u_1(0)=u_2(0), \tag{6a}$$

$$\mu_1\frac{du_1}{dy_1}(0)=\mu_2\frac{du_2}{dy_2}(0) \tag{6b}$$

$$T_1(0)=T_2(0), \tag{6c}$$

$$k_1\frac{dT_1}{dy_1}(0)=k_2\frac{dT_2}{dy_2}(0) \tag{6d}$$

It is seen that the capillary effect between the fluids at the interface is neglected.

Equations (5*a*) and (5*c*) indicate that both fluids do not slip at the walls of the channel. Equations (5*b*) and (5*d*) indicate that both fluids have different temperatures at the walls. Equations (6*a*) and (6*c*) indicate that both fluids have the same velocity and temperature at the interface. Equations (6*b*) and (6*d*) suggest that the shear stress and heat flux of both fluids are continuous across the interface.

It is convenient to nondimensionalize the governing equations and conditions by assuming $T_0 = T_{w2}$ and employing

$$\eta_i = \frac{y_i}{h_i}, \quad F_i = \frac{u_i}{u_1}, \quad \theta_i = \frac{T_i - T_0}{T_{w1} - T_{w2}}, \quad P = \frac{\partial p / \partial x}{\mu_1 \overline{u_1} / h_1^2}, \quad i = 1,2 \tag{7}$$

where $\overline{u_1}$ is the average velocity for Fluid 1. Substituting Eq. (7) into Eqs. (1) through (6) yields the following dimensionless equations and conditions:

$$\frac{d^2 F_1}{d\eta_1^2} - M^2 F_1 - DF_1 - IF_1^2 - P + \frac{\mathrm{Gr}}{\mathrm{Re}}\theta_1 = 0 \tag{8}$$

$$\frac{d^2 \theta_1}{d\eta_1^2} \pm \phi_1 \theta_1 = 0 \tag{9}$$

$$\frac{d^2 F_2}{d\eta_2^2} - Smh^2 M^2 F_2 - h^2 DF_2 - Ih^2 mnF_2^2 - mh^2 P + \beta mnh^2 \frac{\mathrm{Gr}}{\mathrm{Re}}\theta_2 = 0 \tag{10}$$

$$\frac{d^2 \theta_2}{d\eta_2^2} \pm \phi_2 \theta_2 = 0 \tag{11}$$

$$F_1(1) = 0, \quad \theta_1(1) = 1, \quad F_2(-1) = 0, \quad \theta_2(-1) = 0 \tag{12}$$

$$\left.\begin{aligned} F_1(0) = F_2(0), \quad \frac{dF_1(0)}{d\eta_1} = \frac{1}{mh}\frac{dF_2(0)}{d\eta_2} \\ \theta_1(0) = \theta_2(0), \quad \frac{d\theta_1(0)}{d\eta_1} = \frac{1}{kh}\frac{d\theta_2(0)}{d\eta_2} \end{aligned}\right\} \tag{13}$$

where

$$\mathrm{Gr} = \rho g \beta_1 h_1 (T_{w1} - T_{w2})/\mu_1, \quad \mathrm{Re} = \frac{\overline{u_1} h_1}{\mu_1/\rho_1},$$

$$M^2 = \frac{\sigma_1 B_0^2 h_1^2}{\mu_1}, \quad \phi_1 = \frac{Q_1 h_1^2}{k_1},$$

$$S = \frac{\sigma_2}{\sigma_1}, \quad m = \frac{\mu_1}{\mu_2}, \quad h = \frac{h_2}{h_1}, \quad n = \frac{\rho_2}{\rho_1}, \quad \beta = \frac{\beta_2}{\beta_1},$$

$$\phi_2 = \frac{Q_2 h_2^2}{k_2}, \quad k = \frac{k_1}{k_2}, \quad D = \frac{h_1^2}{K}, \quad I = \frac{C_F \overline{u_1} h_1^2}{\mu_1/\rho_1} \tag{14}$$

are the Grashof number, Reynolds number, square of the Hartmann number, dimensionless heat generation or absorption coefficient for Fluid 1, ratio of electrical conductivities, viscosity ratio, ratio of heights, density ratio, ratio of thermal expansion coefficients, dimensionless heat generation or absorption coefficient for Fluid 2, ratio of effective thermal conductivities of the porous medium, inverse Darcy number, and the dimensionless porous medium inertia coefficient, respectively. Setting both D and I equal to zero in Eqs. (8) and (10) corresponds to the case of a nonporous channel.

Equations (8)–(11) are all nonlinear and are coupled through the buoyancy effects and the interface conditions. However, they can be solved analytically if the porous medium inertia effects are neglected (i.e., $I = 0$). In this case, the temperature fields for both fluids are first determined by solving Eqs. (9) and (11) and their solutions are then substituted in Eqs. (8) and (10) to obtain the velocity fields of both phases. The form of the analytical solutions for θ_1 and θ_2 is different depending on whether the signs before ϕ_1 and ϕ_2 are positive or negative. Therefore, two different solutions for θ_1 and θ_2 corresponding to the cases of heat generation fluids ($+\phi_1 > 0, +\phi_2 > 0$) and the heat absorption fluids ($-\phi_1 < 0, -\phi_2 < 0$) are obtained. Obviously, cases where one of the fluids is heat generating and the other one is heat absorbing can be obtained in the same manner. This is not done herein for brevity.

Heat-Generation Case ($+\phi_1 > 0, +\phi_2 > 0$). For this situation and without going into detail the solutions for the temperature fields θ_1 and θ_2 can be shown to be

$$\theta_1(\eta) = \frac{1}{\alpha}\left(\sqrt{\phi_2}\cos\sqrt{\phi_2}\sin\sqrt{\phi_1}\eta + kh\sqrt{\phi_1}\sin\sqrt{\phi_2}\cos\sqrt{\phi_1}\eta\right) \tag{15}$$

$$\theta_2(\eta) = \frac{kh\sqrt{\phi_1}}{\alpha}\left(\cos\sqrt{\phi_2}\sin\sqrt{\phi_2}\eta + \sin\sqrt{\phi_2}\cos\sqrt{\phi_2}\eta\right) \tag{16}$$

where

$$\alpha = kh\sqrt{\phi_1}\sin\sqrt{\phi_2}\cos\sqrt{\phi_1} + \sqrt{\phi_2}\cos\sqrt{\phi_2}\sin\sqrt{\phi_1} \tag{17}$$

The corresponding velocity fields of both fluids F_1 and F_2 can be shown to be

$$F_1(\eta) = C_1\exp(\sqrt{a}\eta) + C_2\exp(-\sqrt{a}\eta) - \frac{bkh\sqrt{\phi_1}}{(\phi_1 + a)\alpha}\sin\sqrt{\phi_2}\cos\sqrt{\phi_1}\eta - \frac{b\sqrt{\phi_2}}{(\phi_1 + a)\alpha}\cos\sqrt{\phi_2}\sin\sqrt{\phi_1} - \frac{c}{a} \tag{18}$$

$$F_2(\eta) = C_3\exp(\sqrt{A}\eta) + C_4\exp(-\sqrt{A}\eta) - \frac{Bkh\sqrt{\phi_1}}{(\phi_2 + A)\alpha}\sin\sqrt{\phi_2}\cos\sqrt{\phi_2}\,\eta - \frac{Bkh\sqrt{\phi_1}}{(\phi_2 + A)\alpha}\cos\sqrt{\phi_2}\sin\sqrt{\phi_2}\eta - \frac{C}{A} \tag{19}$$

where

$$C_1 = \frac{\Delta_1}{\Delta}, \quad C_2 = \frac{\Delta_2}{\Delta}, \quad C_3 = \frac{\Delta_3}{\Delta}, \quad C_4 = \frac{\Delta_4}{\Delta} \tag{20}$$

$$\Delta = \left(\frac{\sqrt{A}}{mh} - \sqrt{a}\right)\left(\exp(\sqrt{A} - \sqrt{a}) - \exp(-(\sqrt{A} - \sqrt{a}))\right) + \left(\frac{\sqrt{A}}{mh} + \sqrt{a}\right)\left(\exp(-(\sqrt{A} + \sqrt{a})) - \exp(\sqrt{A} + \sqrt{a})\right) \tag{21}$$

$$\Delta_1 = -\alpha_2\left(\frac{\sqrt{A}}{mh} - \sqrt{a}\right)\exp(-\sqrt{A}) - \alpha_2\left(\frac{\sqrt{A}}{mh} + \sqrt{a}\right)\exp(\sqrt{A}) + \frac{2\alpha_3\sqrt{A}}{mh}\exp(-\sqrt{a}) + \left(\frac{\alpha_1\sqrt{A}}{mh} + \alpha_4\right)\exp(-(\sqrt{A} + \sqrt{a})) + \left(\frac{\alpha_1\sqrt{A}}{mh} - \alpha_4\right)\exp(\sqrt{A} - \sqrt{a}) \tag{22}$$

$$\Delta_2=\frac{-2\alpha_3\sqrt{A}}{mh}\exp\sqrt{a}-\left(\frac{\alpha_1\sqrt{A}}{mh}+\alpha_4\right)\exp(-(\sqrt{A}-\sqrt{a}))$$
$$-\left(\frac{\alpha_1\sqrt{A}}{mh}-\alpha_4\right)\exp(\sqrt{A}+\sqrt{a})+\alpha_2\left(\frac{\sqrt{A}}{mh}+\sqrt{a}\right)\exp(-\sqrt{A})$$
$$+\alpha_2\left(\frac{\sqrt{A}}{mh}-\sqrt{a}\right)\exp(\sqrt{A}) \tag{23}$$

$$\Delta_3=-\alpha_3\left(\frac{\sqrt{A}}{mh}-\sqrt{a}\right)\exp(\sqrt{a})+\alpha_3\left(\frac{\sqrt{A}}{mh}+\sqrt{a}\right)\exp(-\sqrt{a})$$
$$+(\alpha_4+\alpha_1\sqrt{a})\exp(\sqrt{A}+\sqrt{a})-(\alpha_4-\alpha_1\sqrt{a})\exp(\sqrt{A}-\sqrt{a})$$
$$-2\alpha_2\sqrt{a}\exp(\sqrt{A}) \tag{24}$$

$$\Delta_4=-\alpha_3\left(\frac{\sqrt{A}}{mh}+\sqrt{a}\right)\exp(\sqrt{a})+\alpha_3\left(\frac{\sqrt{A}}{mh}-\sqrt{a}\right)\exp(-\sqrt{a})$$
$$-(\alpha_4+\alpha_1\sqrt{a})\exp(-(\sqrt{A}-\sqrt{a}))+(\alpha_4-\alpha_1\sqrt{a})$$
$$\times\exp(-(\sqrt{A}+\sqrt{a}))+2\alpha_2\sqrt{a}\exp(-\sqrt{A}) \tag{25}$$

$$\alpha_1=\frac{bkh\sqrt{\phi_1}}{(\phi_1+a)\alpha}\sin\phi_2-\frac{Bkh\sqrt{\phi_1}}{(\phi_2+A)\alpha}\sin\sqrt{\phi_2}+\frac{c}{a}-\frac{C}{A} \tag{26}$$

$$\alpha_2=\frac{bkh\sqrt{\phi_1}}{(\phi_1+a)\alpha}\sin\sqrt{\phi_2}\cos\sqrt{\phi_1}$$
$$+\frac{b\sqrt{\phi_2}}{(\phi_1+a)\alpha}\cos\sqrt{\phi_2}\sin\sqrt{\phi_1}+\frac{c}{a} \tag{27}$$

$$\alpha_3=\frac{C}{A},\quad \alpha_4=-\frac{Bkh\sqrt{\phi_1}\sqrt{\phi_2}}{mh(\phi_2+A)\alpha}\cos\sqrt{\phi_2}+\frac{b\sqrt{\phi_1}\sqrt{\phi_2}}{(\phi_1+a)\alpha}\cos\sqrt{\phi_2} \tag{28}$$

$$a=M^2+D,\quad b=-\frac{\mathrm{Gr}}{\mathrm{Re}},\quad c=P,\quad A=Smh^2M+h^2D \tag{29}$$

$$B=-\beta mnh^2\frac{\mathrm{Gr}}{\mathrm{Re}},\quad C=mh^2P$$

It should be noted that in Eqs. (15)–(19), η is in the range such that $0\leqslant\eta\leqslant1$ for θ_1 and F_1 and $-1\leqslant\eta\leqslant0$ for θ_2 and F_2.

Heat-Absorption Case ($-\phi_1<0,-\phi_2<0$). In a similar fashion as in the case of $+\phi_1>0$ and $+\phi_2>0$, the solutions for this case can be obtained. Again, for brevity and without going into detail, the temperature and velocity profiles of both fluids can be shown to be

$$\theta_1(\eta)=C_5\exp(\sqrt{\phi_1}\eta)+C_6\exp(-\sqrt{\phi_1}\eta) \tag{30}$$

$$\theta_2(\eta)=C_7\exp(\sqrt{\phi_2}\eta)+C_8\exp(-\sqrt{\phi_2}\eta) \tag{31}$$

where

$$C_5=\frac{\Delta_5}{\Delta^*},\quad C_6=\frac{\Delta_6}{\Delta^*},\quad C_7=\frac{\Delta_7}{\Delta^*},\quad C_8=\frac{\Delta_8}{\Delta^*} \tag{32}$$

$$\Delta^*=-\left(\frac{\sqrt{\phi_2}}{kh}-\sqrt{\phi_1}\right)\exp(\sqrt{\phi_1}-\sqrt{\phi_2})-\left(\frac{\sqrt{\phi_2}}{kh}+\sqrt{\phi_1}\right)$$
$$\times\exp(\sqrt{\phi_1}-\sqrt{\phi_2})+\left(\frac{\sqrt{\phi_2}}{kh}+\sqrt{\phi_1}\right)\exp(-(\sqrt{\phi_1}+\sqrt{\phi_2}))$$
$$+\left(\frac{\sqrt{\phi_2}}{kh}-\sqrt{\phi_1}\right)\exp(-(\sqrt{\phi_1}-\sqrt{\phi_2})) \tag{33}$$

$$\Delta_5=-\left(\frac{\sqrt{\phi_2}}{kh}-\sqrt{\phi_1}\right)\exp(-\sqrt{\phi_2})-\left(\frac{\sqrt{\phi_2}}{kh}+\sqrt{\phi_1}\right)\exp(\sqrt{\phi_2}) \tag{34}$$

$$\Delta_6=\left(\frac{\sqrt{\phi_2}}{kh}+\sqrt{\phi_1}\right)\exp(-\sqrt{\phi_2})-\left(\frac{\sqrt{\phi_2}}{kh}-\sqrt{\phi_1}\right)\exp(\sqrt{\phi_2}) \tag{35}$$

$$\Delta_7=2\sqrt{\phi_1}\exp(\sqrt{\phi_2}),\quad \Delta_8=2\sqrt{\phi_1}\exp(-\sqrt{\phi_2}) \tag{36}$$

$$F_1(\eta)=C_9\exp(\sqrt{a}\eta)+C_{10}\exp(-\sqrt{a}\eta)+\frac{bC_5}{\phi_1-a}\exp(\sqrt{\phi_1}\eta)$$
$$+\frac{bC_6}{\phi_1-a}\exp(-\sqrt{\phi_1}\eta)+\frac{c}{a} \tag{37}$$

$$F_2(\eta)=C_{11}\exp(\sqrt{A}\eta)+C_{12}\exp(-\sqrt{A}\eta)+\frac{BC_7}{\phi_2-A}\exp(\sqrt{\phi_2}\eta)$$
$$+\frac{BC_8}{\phi_2-A}\exp(-\sqrt{\phi_2}\eta)+\frac{C}{A} \tag{38}$$

where

$$C_9=\frac{\Delta_9}{\Delta^{**}},\quad C_{10}=\frac{\Delta_{10}}{\Delta^{**}},\quad C_{11}=\frac{\Delta_{11}}{\Delta^{**}},\quad C_{12}=\frac{\Delta_{12}}{\Delta^{**}} \tag{39}$$

$$\Delta^{**}=-\left(\frac{\sqrt{A}}{mh}-\sqrt{a}\right)\exp(\sqrt{a}-\sqrt{A})-\left(\frac{\sqrt{A}}{mh}+\sqrt{a}\right)\exp(\sqrt{a}+\sqrt{A})$$
$$+\left(\frac{\sqrt{A}}{mh}+\sqrt{a}\right)\exp(-(\sqrt{a}+\sqrt{A}))+\left(\frac{\sqrt{A}}{mh}-\sqrt{a}\right)$$
$$\times\exp(-(\sqrt{a}-\sqrt{A})) \tag{40}$$

$$\Delta_9=-\gamma_2\left(\frac{\sqrt{A}}{mh}-\sqrt{a}\right)\exp(-\sqrt{A})-\gamma_2\left(\frac{\sqrt{A}}{mh}+\sqrt{a}\right)\exp(\sqrt{A})$$
$$+\frac{2\gamma_3\sqrt{A}}{mh}\exp(-\sqrt{a})+\left(\frac{\gamma_1\sqrt{A}}{mh}+\gamma_4\right)\exp(-(\sqrt{A}+\sqrt{a}))$$
$$+\left(\frac{\gamma_1\sqrt{A}}{mh}-\gamma_4\right)\exp(\sqrt{A}-\sqrt{a}) \tag{41}$$

$$\Delta_{10}=\frac{-2\gamma_3\sqrt{A}}{mh}\exp(\sqrt{a})-\left(\frac{\gamma_1\sqrt{A}}{mh}+\gamma_4\right)\exp(-(\sqrt{A}-\sqrt{a}))$$
$$-\left(\frac{\gamma_1\sqrt{A}}{mh}-\gamma_4\right)\exp(\sqrt{A}+\sqrt{a})+\gamma_2\left(\frac{\sqrt{A}}{mh}+\sqrt{a}\right)\exp(-\sqrt{A})$$
$$+\gamma_2\left(\frac{\sqrt{A}}{mh}-\sqrt{a}\right)\exp(\sqrt{A}) \tag{42}$$

$$\Delta_{11}=-\gamma_3\left(\frac{\sqrt{A}}{mh}-\sqrt{a}\right)\exp(\sqrt{a})+\gamma_3\left(\frac{\sqrt{A}}{mh}+\sqrt{a}\right)\exp(-\sqrt{a})$$
$$+(\gamma_4+\gamma_1\sqrt{a})\exp(\sqrt{A}+\sqrt{a})-(\gamma_4-\gamma_1\sqrt{a})\exp(\sqrt{A}-\sqrt{a})$$
$$-2\gamma_2\sqrt{a}\exp(\sqrt{A}) \tag{43}$$

$$\Delta_{12}=-\gamma_3\left(\frac{\sqrt{A}}{mh}+\sqrt{a}\right)\exp(\sqrt{a})+\gamma_3\left(\frac{\sqrt{A}}{mh}-\sqrt{a}\right)\exp(-\sqrt{a})$$
$$-(\gamma_4+\gamma_1\sqrt{a})\exp(-(\sqrt{A}-\sqrt{a}))+(\gamma_4-\gamma_1\sqrt{a})$$
$$\times\exp(-(\sqrt{A}+\sqrt{a}))+2\gamma_2\sqrt{a}\exp(-\sqrt{A}) \tag{44}$$

$$\gamma_1=\frac{-b(C_5+C_6)}{\phi_1-a}+\frac{B(C_7+C_8)}{\phi_2-A}+\frac{c}{a}-\frac{C}{A} \tag{45}$$

$$\gamma_2=\frac{-bC_5}{\phi_1-a}\exp(\sqrt{\phi_1})-\frac{bC_6}{\phi_1-a}\exp(-\sqrt{\phi_1})+\frac{c}{a} \tag{46}$$

$$\gamma_3 = \frac{-BC_7}{\phi_2 - A}\exp(-\sqrt{\phi_2}) - \frac{BC_8}{\phi_2 - A}\exp(\sqrt{\phi_2}) + \frac{C}{A} \quad (47)$$

$$\gamma_4 = \frac{b\sqrt{\phi_1}}{\phi_1 - a}(C_6 - C_5) + \frac{B\sqrt{\phi_2}}{mh(\phi_2 - A)}(C_7 - C_8) \quad (48)$$

Results and Discussion

Numerical evaluation of the analytical solutions reported before are performed and the results are illustrated graphically in Figs. 2–13 to show interesting features of the solutions. In addition, numerical solutions based on the standard implicit finite-difference methodology discussed by Blottner [24] are also reported for comparison purposes with the above analytical solutions and previously published work.

In Fig. 2, a comparison of the velocity profiles obtained analytically and numerically for different magnetic Hartmann num-

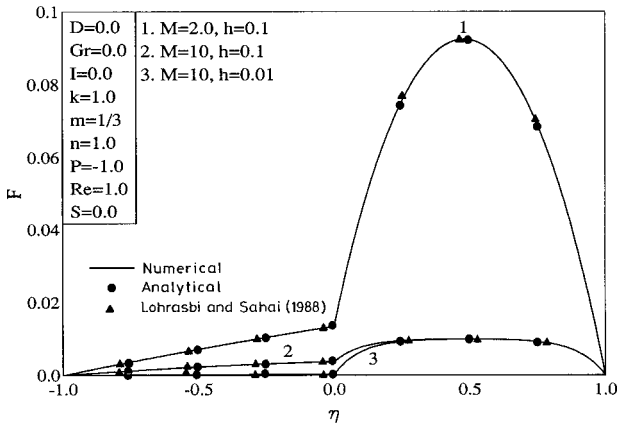

Fig. 2 Comparison of velocity profiles

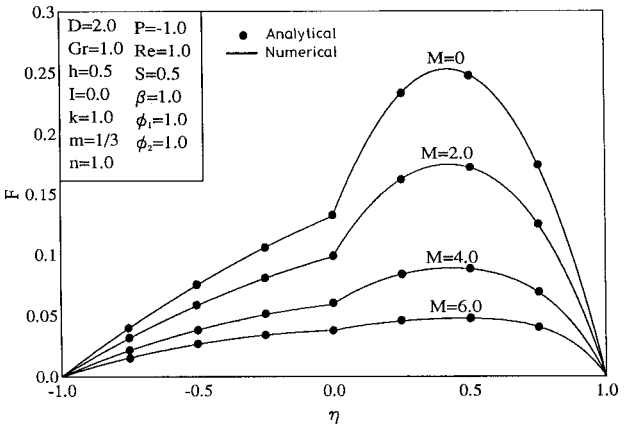

Fig. 3 Effects of M on velocity profiles

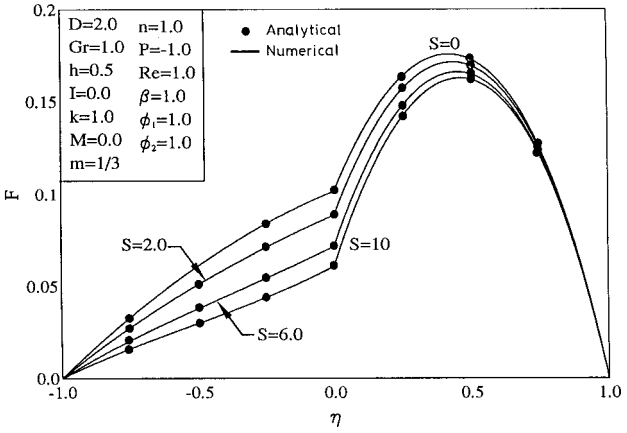

Fig. 4 Effects of *S* on velocity profiles

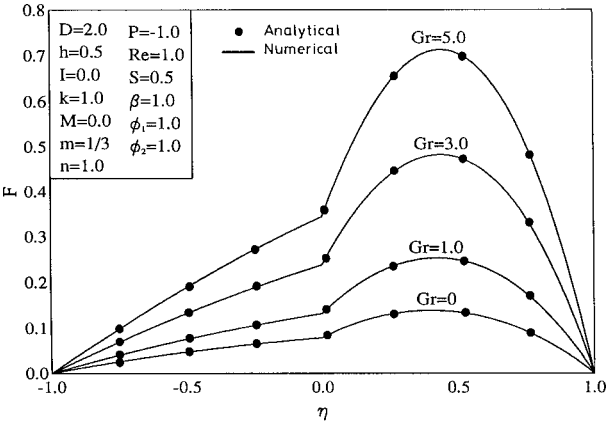

Fig. 5 Effects of Gr on velocity profiles

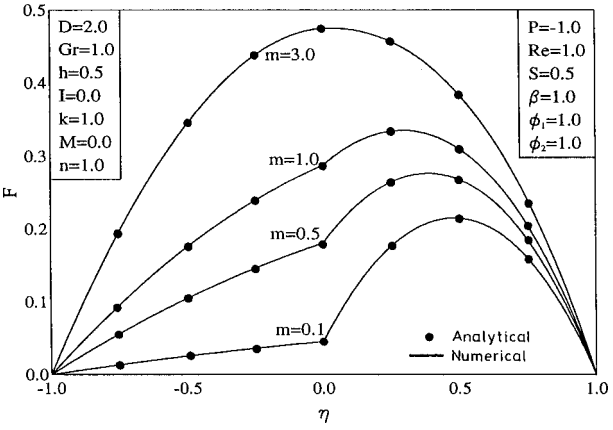

Fig. 6 Effects of *m* on velocity profiles

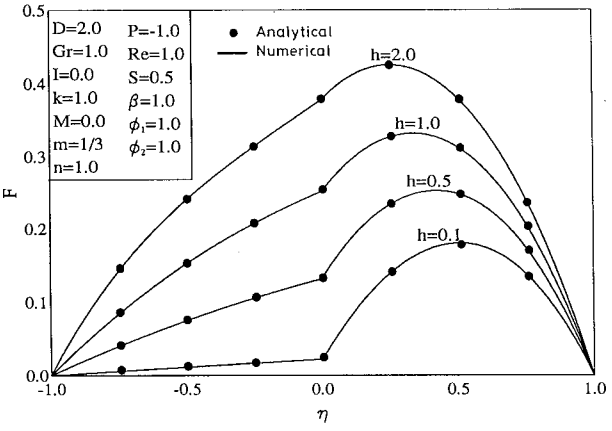

Fig. 7 Effects of *h* on velocity profiles

In Fig. 2, a comparison of the velocity profiles obtained analytically and numerically for different magnetic Hartmann num-

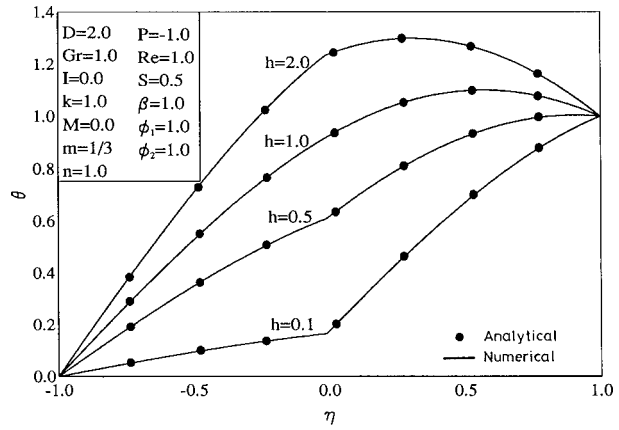

Fig. 8 Effects of *h* on temperature profiles

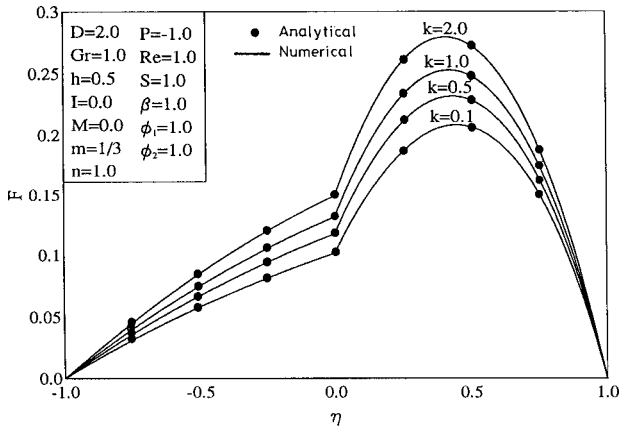

Fig. 11 Effects of *k* on velocity profiles

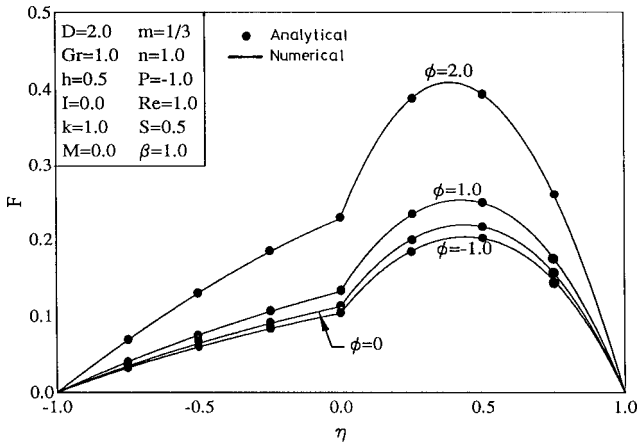

Fig. 9 Effects of ϕ on velocity profiles

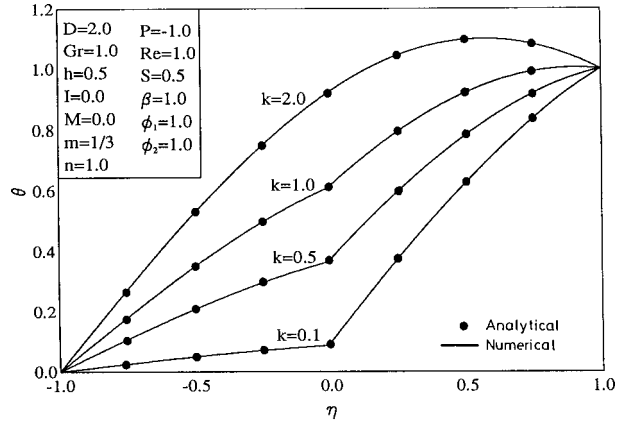

Fig. 12 Effects of *k* on temperature profiles

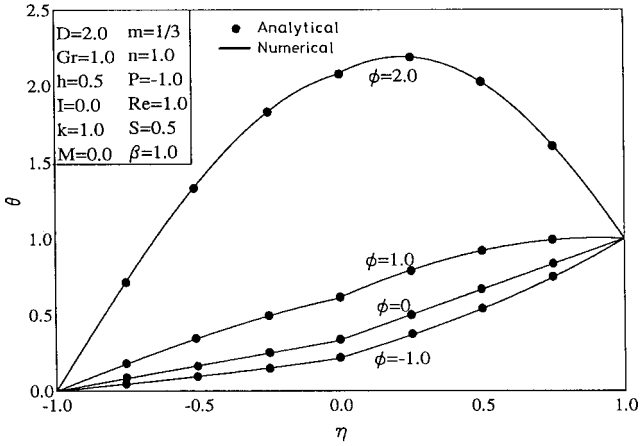

Fig. 10 Effects of ϕ on temperature profiles

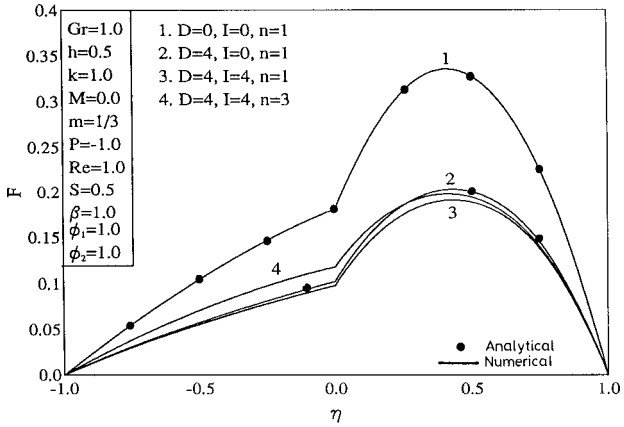

Fig. 13 Effects of *D*, *I*, and *n* on velocity profiles

bers M and height ratios with those reported earlier by Lohrasbi and Sahai [5] is displayed. It is obvious from this figure that excellent agreement between the results exists. This lends confidence in both the analytical and numerical results to be reported subsequently.

Figures 3 and 4 present typical velocity profiles for both fluids in the channel for various values of the Hartmann number M and the ratio of the electrical conductivities *S*, respectively. It should be noted that, in these and all subsequent figures for the velocity distributions, F corresponds to F_2 in the range $-1 \leqslant \eta \leqslant 0$ and corresponds to F_1 in the range of $0 \leqslant \eta \leqslant 1$. The continuity condi-

tion for the velocities of both fluids is evident at $\eta=0$. Physically speaking, application of a magnetic field normal to the flow direction gives rise to a resistive force called the Lorentz force which acts in the direction opposite to that of the flow. This has the tendency to slow down the movement of the fluids in the channel. Increasing the magnetic field strength yields an increase in the effect of the Lorentz force which results in a further decrease in the velocities of the fluids. Furthermore, increasing the ratio of the electrical conductivities of the fluids such that $S>1$ causes further reductions in the flow movement in the channel with more effect on Fluid 2 since it has a higher electrical conductivity and, therefore, is affected more by the presence of the magnetic field. All of these behaviors are evident by the decreases in F as either M or S is increased.

Figures 5 and 6 illustrate the influence of inclusion of the buoyancy effects ($\mathrm{Gr}\neq 0$) and increasing the viscosity ratio (m) of both fluids, respectively. The presence of the buoyancy effects ($\mathrm{Gr}>0$) complicates the problem through coupling of the flow problem with the thermal problem for both fluids which are already coupled through the matching or continuity conditions at $\eta=0$. Physically, the presence of the thermal buoyancy currents induces more flow in the channel which is taking place through the application of a pressure gradient. Thus, increasing the value of the Grashof number Gr produces increases in the velocities of both fluids as is obvious from Fig. 5. Also, increases in the values of the viscosity ratio m result in enhancement of the velocity fields of both fluids. For large values of m ($m=3$) both fluids move in the channel with almost symmetrical velocity profiles for which their maximum velocity occurs almost at the interface ($\eta=0$). This is clear from Fig. 6.

Figures 7 and 8 depict the effect of the height ratio h on the velocity and temperature distributions of both fluids in the channel, respectively. In these figures, increases in the height ratio h is observed to produce increases in both the velocity and temperature distributions in the vertical channel. For large values of h, the velocity profiles for both fluids are becoming almost symmetric about the interface line ($\eta=0$).

The influence of the heat generation or absorption coefficients of both fluids ϕ_1 and ϕ_2 on the velocity and temperature profiles are given in Figs. 9 and 10, respectively. In these and all previous and subsequent figures, it is taken $\phi_1=\phi_2=\phi$ in order to minimize the number of figures. Heat generation of both fluids ($\phi>0$) has the tendency to increase the temperatures of the fluids. Therefore, for $\mathrm{Gr}>0$ the buoyancy effects increase which, as mentioned before, results in higher fluid velocities in the channel. Conversely, heat absorption of both fluids ($\phi<0$) causes the opposite effect, namely decreases in the velocity and temperature fields of both fluids. These facts are clearly shown in Figs. 9 and 10.

Figures 11 and 12 display the effects of the thermal conductivity ratio k on the velocity and temperature distributions of both fluids in the channel. It is seen from these figures that increasing the value of k enhances the temperatures of both fluids and that the almost linear temperature profiles for small values of k become nonlinear for large values of k. Due to the thermal buoyancy effects, this produces enhanced flow velocities in the channel.

Finally, in Fig. 13, the influence of the presence of the porous medium Darcian ($\mathrm{D}\neq 0$) and inertial ($I\neq 0$) effects as well as the fluids density ratio n on the velocity distributions in the channel is illustrated. These results are obtained numerically. It is observed that similar to the magnetic field, the presence of the porous medium produces flow resistance effects. In addition, the inertia effect adds on this resistance mechanism which further reduces the flow in the channel. Furthermore, increasing the density ratio n is also seen to enhance the flow of both fluids in the porous channel.

As shown in all of the above discussed graphical figures, excellent agreement between the numerical results and the analytical solutions reported earlier is obtained. This confirms the correctness of the analytical solutions and the accuracy of the numerical results.

Conclusion

The problem of steady, laminar, hydromagnetic flow and heat transfer of two immiscible fluids in a vertical channel of asymmetric wall temperatures filled with a uniform porous medium and in the presence of free convection currents was considered. The governing equations for this investigation were derived and proper dimensionless parameters are employed. The coupled dimensionless equations were solved analytically for the velocity and temperature profiles of both fluids for the case where the inertia effects of the porous medium are neglected. Numerical evaluations of the analytical solutions were performed and the results were illustrated graphically for various parametric conditions. When the porous medium inertia effects are included, the problem is solved numerically by an accurate implicit finite-difference technique. The numerical results were successfully validated by the obtained analytical solutions. In addition, excellent agreement with previously published work was obtained. It was found that, the presence of buoyancy effects, and heat generation enhances the flow rate in the porous medium channel while the opposite is true for heat absorption. Increases in the values of the Hartmann number, the inverse Darcy number, and the electrical conductivity ratio produced reduced flow velocities in the channel while increases in the viscosity ratio, density ratio, thermal conductivity ratio, and the height ratio of both fluids increased the flow in the porous medium channel. The thermal aspects of the fluids in the channel were enhanced by increases in the height ratio, heat generation coefficient, and the thermal conductivity ratio of both fluids. It is hoped that the physical behavior of two-immiscible fluids flow through porous and non-porous channels illustrated in the present work can be used as a vehicle for understanding the effect of slag layers and heat generation on the performance of coal-fired MHD generators and the process of hydrocarbon recovery from underground petroleum deposits.

Acknowledgment

The author acknowledges and thanks the financial support of the Research Administration at Kuwait University through the Research Grant No. EM-121.

Nomenclature

- B_o = magnetic induction
- C_F = porous medium inertia coefficient
- D = inverse Darcy number ($\mathrm{D}=h_1^2/K$)
- F_i = dimensionless velocity ($F_i=u_i/u_1, i=1,2$)
- g = gravitational acceleration
- Gr = Grashof number ($\mathrm{Gr}=\rho g\beta_1 h_1(T_{w1}-T_{w2})/\mu_1$)
- h = ratio of fluids heights ($h=h_2/h_1$)
- h_i = height of fluid i, $i=1,2$.
- I = dimensionless porous medium inertia coefficient ($I=C_F\overline{u}_1 h_1^2\rho_1/\mu_1$)
- k = ratio of effective thermal conductivities ($k=k_1/k_2$)
- k_i = effective thermal conductivity of fluid i, $i=1,2$.
- K = permeability of porous medium
- m = dynamic viscosity ratio ($m=\mu_1/\mu_2$)
- M = Hartmann number ($\mathrm{M}^2=\sigma_1 B_0^2 h_1^2/\mu_1$)
- n = density ratio ($n=\rho_2/\rho_1$)
- p = dimensional pressure
- P = dimensionless pressure gradient ($P=(\partial p/\partial x)h_1^2/(\mu_1\overline{u}_1)$)
- Q_i = dimensional heat generation or absorption of fluid i, $i=1,2$.
- Re = Reynolds number ($\mathrm{Re}=\rho_1\overline{u}_1 h_1/\mu_1$)
- S = ratio of electrical conductivities ($S=\sigma_2/\sigma_1$)
- T = dimensional temperature
- u = dimensional velocity
- $\overline{u}$ = average velocity
- x = vertical distance
- y = normal distance

β = ratio of thermal expansion coefficients ($\beta = \beta_2/\beta_1$)
β_i = thermal expansion coefficient of fluid i, $i = 1,2$.
η = dimensionless normal distance ($\eta_i = y_i/h_i$, $i = 1,2$)
ϕ = dimensionless heat generation or absorption coefficient ($\phi = Qh/k$)
μ = fluid dynamic viscosity
μ_e = effective dynamic viscosity
ρ = fluid density
σ = fluid electrical conductivity
θ = dimensionless temperature ($\theta = (T_i = T_o)(T_{w1} - T_{w2})$, $i = 1,2$)

Subscripts

1 = fluid 1
2 = fluid 2
w = wall

References

[1] Pian, Carlson C., and Smith, J. M., 1977, ''Velocity and Temperature Distributions of Coal-Slag Layers on Magnetohydrodynamic Generator Walls,'' NASA TN D-8396.
[2] Shail, R., 1973, ''On Laminar Two-Phase Flow in Magnetohydrodynamics,'' Int. J. Eng. Sci., **11**, pp. 1103–1108.
[3] Thome, R. J., 1964, ''Effect of Transverse Magnetic Field on Vertical Two-Phase Flow Through a Rectangular Channel,'' Argonne National Laboratory Report No. ANL 6854.
[4] Postlethwaite, A. W., and Sluyter, M. M., 1978, ''MHD Heat Transfer Problems—An Overview,'' ASME, Mechanical Engineering, **100**, pp. 32–39.
[5] Lohrasbi, J., and Sahai, V., 1988, ''Magnetohydrodynamic Heat Transfer in Two-Phases Flow Between Parallel Plates,'' Appl. Sci. Res., **45**, pp. 53–66.
[6] Malashetty, M. S., and Leela, V., 1991, ''Magnetohydrodynamic Heat Transfer in Two Fluid Flow,'' *Proceedings of the National Heat Transfer*, Conf. AIChE & ASME, HTD, p. 159.
[7] Malashetty, M. S., and Leela, V., 1992, ''Magnetohydrodynamic Heat Transfer in Two Phase Flow,'' Int. J. Eng. Sci., **30**, pp. 371–377.
[8] Malashetty, M. S., and Umavathi, J. C., 1997, ''Two-Phase Magnetohydrodynamic Flow and Heat Transfer in an Inclined Channel,'' Int. J. Multiphase Flow, **23**, pp. 545–560.
[9] Hiremath, P. S., and Patil, P. M., 1993, ''Free Convection Effects on the Oscillatory Flow of a Couple Stress Fluid Through a Porous Medium,'' Acta Mech., **98**, pp. 143–158.
[10] Vafai, K., and Tien, C. L., 1981, ''Boundary and Inertia Effects on Flow and Heat Transfer in Porous Media,'' Int. J. Heat Mass Transf., **24**, pp. 195–203.
[11] Plumb, O. A., and Huenefeld, J. C., 1981, ''Non-Darcy Natural Convection from Heated Surfaces in Saturated Porous Media,'' Int. J. Heat Mass Transf., **24**, pp. 765–768.
[12] Nakayama, A., Koyama, H., and Kuwahara, F., 1988, ''An Analysis on Forced Convection in a Channel Filled with a Brinkman-Darcy Porous Medium: Exact and Approximate Solutions,'' Warme-und Stoffubertragung, **23**, pp. 291–95.
[13] Renken, K. J., and Poulikakos, D., 1988, ''Experiment and Analysis of Forced Convective Heat Transport in a Packed Bed of Spheres,'' Int. J. Heat Transf., **31**, pp. 1399–1408.
[14] Vafai, K., and Kim, S., 1989, ''Forced Convection in a Channel Filled with a Porous Medium: An Exact Solution,'' ASME J. Heat Transfer, **111**, pp. 1103–1106.
[15] Srinivasan, V., and Vafai, K., 1994, ''Analysis of Linear Encroachment in Two-Immiscible Fluid Systems,'' ASME J. of Fluids Engineering, **116**, pp. 135–139.
[16] Chen, S. C., and Vafai, K., 1996, ''Analysis of Free Surface Momentum and Energy Transport in Porous Media,'' Numer. Heat Transfer, Part A, **29**, pp. 281–296.
[17] Chen, S. C., and Vafai, K., 1997, ''Non-Darcian Surface Effects on Free Surface Transport in Porous Media,'' Numer. Heat Transfer, Part A, **31**, pp. 235–254.
[18] Cramer, K. R., and Pai, S.-I., 1973, ''Magnetofluid Dynamics for Engineers and Applied Physicists, Scripta Publishing, Washington, D.C.
[19] Sparrow, E. M. and Cess, R. D., 1961, ''Temperature Dependent Heat Sources or Sinks in a Stagnation Point Flow,'' Appl. Sci. Res., **A10**, pp. 185–197.
[20] Vajravelu, K., and Nayfeh, J., 1992, ''Hydromagnetic Convection at a Cone and a Wedge,'' Int. Commun. Heat Mass Transfer, **19**, pp. 701–710.
[21] Vajravelu, K., and Hadjinicolaou, A., 1993, ''Heat Transfer in a Viscous Fluid Over a Stretching Sheet with Viscous Dissipation and Internal Heat Generators,'' Int. Commun. Heat Mass Transfer, **20**, pp. 417–430.
[22] Chamkha, A. J., 1997, ''Non-Darcy Fully Developed Mixed Convection in a Porous Medium Channel with Heat Generation/Absorption and Hydromagnetic Effects,'' Numer. Heat Transfer, Part A, **32**, pp. 853–875.
[23] Song, T. H., 1996, ''Stability of a Fluid Layer with Uniform Heat Generation and Convection Boundary Conditions,'' Int. J. Heat Mass Transf., **39**, pp. 2378–2382.
[24] Blottner, F., 1970, ''Finite-Difference Methods of Solution of the Boundary-Layer Equations,'' AIAA J., **8**, pp. 193–205.